# A METHOD FOR INCREASING PRECISION AND RELIABILITY OF ELASTICITY ANALYSIS IN COMPLICATED BURN SCAR CASES*

LEONID V. TSAP

*Lawrence Livermore National Laboratory*
*Center for Applied Scientific Computing*
*Livermore, CA 94551, USA*
*E-mail: tsap@llnl.gov*

DMITRY B. GOLDGOF and SUDEEP SARKAR

*Department of Computer Science and Engineering*
*University of South Florida*
*Tampa, FL 33620, USA*
*E-mail: {goldgof, sarkar}@csee.usf.edu*

PAULINE S. POWERS

*Department of Psychiatry/Tampa Bay Regional Burn Center*
*University of South Florida*
*Tampa, FL 33620, USA*

In this paper we propose a method for increasing precision and reliability of elasticity analysis in complicated burn scar cases. The need for a technique that would help physicians by objectively assessing elastic properties of scars, motivated our original algorithm. This algorithm successfully employed active contours for tracking and finite element models for strain analysis. However, the previous approach considered only one normal area and one abnormal area within the region of interest, and scar shapes which were somewhat simplified. Most burn scars have rather complicated shapes and may include multiple regions with different elastic properties. Hence, we need a method capable of adequately addressing these characteristics. The new method can split the region into more than two localities with different material properties, select and quantify abnormal areas, and apply different forces if it is necessary for a better shape description of the scar. The method also demonstrates the application of scale and mesh refinement techniques in this important domain. It is accomplished by increasing the number of Finite Element Method (FEM) areas as well as the number of elements within the area.

The method is successfully applied to elastic materials and real burn scar cases. We demonstrate all of the proposed techniques and investigate the behavior of elasticity function in a 3-D space. Recovered properties of elastic materials are compared with those obtained by a conventional mechanics-based approach. Scar ratings achieved with the method are correlated against the judgments of physicians.

*Keywords*: Physically-based vision; deformable models; nonrigid motion analysis; active contours; biomedical applications; iterative descent search; finite element analysis.

*This research was supported in part by the Whitaker Foundation Biomedical Engineering Research Grant and in part by the National Science Foundation Grants IRI-9619240, EIA-9729904 and CDA-9724422. The work was performed at the University of South Florida as a part of the dissertation research.



International Journal of Pattern Recognition and Artificial Intelligence, Vol. 14, No. 2 (2000) 189–211

## 1. INTRODUCTION

Burn scar assessment is a very important problem. Two million people are burned annually in the United States and 300,000 are seriously injured.[21] Along with advances in the understanding of the process of scar formation, recent years have seen progress in the therapeutic treatment of scars. The treatment procedures include using various types of pressure garments, drugs, or even surgery. Despite various new developments in terms of reducing scars or their impact, the ability to *objectively* assess scars is still very limited. Presently, the specialists at the Tampa General Hospital Burn Center characterize burn scars using a scale similar to the Vancouver Burn Scar Assessment questionnaire which asks the surgeons to rate properties of the scar on a coarse scale. Obviously, this involves the subjective judgment of the specialist and it was found that the reliability of these ratings is not adequate. The same surgeon might rate the same scar differently at different times. Also, different surgeons might rate the same scar differently. In the interest of making the best choice for the patient, physicians need to be able to compare and contrast various healing techniques both subjectively and objectively.

This paper presents a set of algorithms for objectively determining the elasticity of multiple burn scars relative to the surrounding areas. The skin elasticity can determine not only the objective parameters of the scar, but also the success of the healing process. The need for technique that would help physicians by objectively assessing elastic properties of scars motivated our original algorithm.[28,29] This algorithm successfully employed active contours for tracking and finite element models for strain analysis. However, the previous approach considered only one normal area and one abnormal area within the region of interest, and simplified scar shapes. Most burn scars have rather complicated shapes and may include multiple regions with different elastic properties. The method proposed in this paper is capable of adequately addressing these characteristics.

### 1.1. Previous Work

This section presents a short review of the previous work in related areas. For a more detailed review see Ref. 29. In computer vision, physically-based modeling is often used for tracking and motion analysis. Terzopoulos and Metaxas[20] presented a physically-based approach to shape modeling that simultaneously satisfies the requirements of reconstruction and recognition. DeCarlo and Metaxas[6] proposed to incorporate blending into deformable models. Sclaroff and Pentland[22] used FEM to obtain a parametric description of nonrigid motion in terms of its similarity to known extremal views. Young and Axel[33] built a finite element model of the left ventricle to fit material points tracked in biplanar views. Metaxas and Koh[19] used local adaptive finite elements to represent 3-D shapes efficiently. Davis *et al.*[5] designed the Elastic Body Spline (EBS) to approximate behavior of a homogeneous, isotropic, elastic material subjected to a load. A finite element model that learns the correct physical model of human lips by training from real data was proposed by Basu and Pentland.[2] Martin *et al.*[16] employed finite element computation of

analytic modes describing shape variation of structures within the human brain. Tsap *et al.*[27,28] first suggested the use of nonlinear FEM for nonrigid motion analysis of human skin containing abnormalities (such as scars).

Active contour models, or snakes, were first introduced by Kass *et al.*[11] as a mechanism for finding and tracking salient image contours. Terzopoulos and Waters[26] developed snakes to track the nonrigid motions of facial features in video images. Kumar and Goldgof[13] used active contours (snakes) to track the tagged grid in Cardiac MR images automatically. McEachen II and Duncan[17] tracked feature points over an entire cardiac cycle. Yezzi *et al.*[32] unified the curve evolution approaches for active contours and the established energy formulation. Gunn and Nixon[8] used two contours to search the image space from both inside and outside of the target feature. Tagare[25] proposed a formulation that achieves reduction in the search space by precomputing orthogonal curves to deform the template. Chandran and Potty[4] developed a strategy to avoid local minimas as a dynamic programming solution for snake energy minimization. Amini *et al.*[1] applied coupled B-spline snake grids to magnetic resonance images and validated results with a 3-D cardiac motion model. Recent developments in deformable model techniques are summarized in Ref. 23.

There is very little work in the area of objective assessment of burn scars. Previously, scar evaluation has been mainly subjective. Sullivan *et al.*[24] addressed the issue of a reliable, objective and universal method of scar rating based on pigmentation, vascularity and scar height. This approach is known as the Vancouver Scar Assessment Technique and is commonly used by plastic surgeons. However, the methodology has some subjective aspects to it, e.g. in comparing skin colors.

Another related area is the work in biomechanical properties of the skin and soft tissue. There has been a significant amount of work in characterizing the material properties of the skin and its relations to movement. The models range from plane geometric models based on continuum mechanics[7] to finite element based methods.[14] Hyperelastic constitutive models have been shown to be appropriate to represent the material behavior of soft tissues.[30] Kallel and Bertrand[12] introduced a method to reconstruct the elastic modulus of a compressed soft tissue using simulated data. However, these techniques have not been applied to the study of burn scar recovery. McHugh *et al.*[18] examined biomechanical changes after burn injury when normal skin attempts to compensate for scar contraction. The authors stressed that more precise measurements are needed to quantify these changes as well as the effects of burn scar treatment.

### 1.2. Overview

Our experimental setup includes a structured light K2T scanner made by K2T Inc. (Duquesne, PA). We stamp a grid pattern on the skin region of interest and then observe the distortion of this pattern upon pulling the skin in a certain direction. Each image sequence consists of both intensity and range images (Fig. 1) before and after the application of a force.

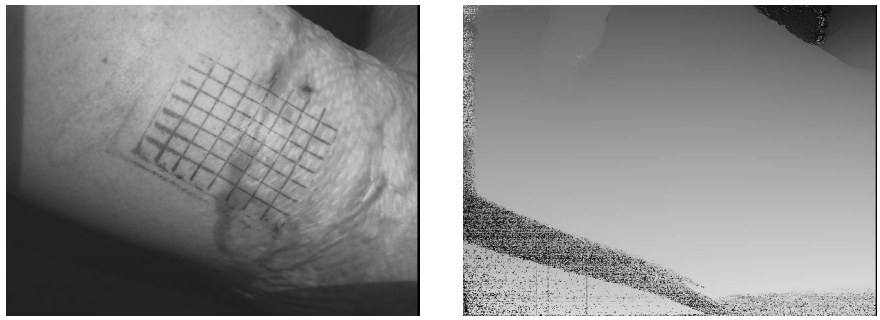

(a) (b)

Fig. 1. (a) Intensity and (b) range images of the skin with the grid. Distances in the range image are encoded as intensities.

Our experiments involve not only skin, but also elastic materials with properties recovered by a conventional mechanics-based method (Sec. 2.1). The new method, similarly to the original,[28,29] employs snakes to detect grid intersections in images before and after stretching (Sec. 2.2). The next step involves initial detection of abnormalities using strain distributions synthesized by the Finite Element Method (FEM). Our nonlinear FEM approach is described in Sec. 2.3. The method uses an iterative descent search outlined in Sec. 2.4 to approximate stretching behavior of the region of interest.

However, the previous approach (described in Sec. 3.1) considered only one normal area and one abnormal area within the region of interest, and scar shapes which were somewhat simplified. The new method, capable of precisely addressing properties of multiple abnormal areas, is presented in detail in Sec. 3.2. The method also addresses application of multiple forces in different directions and mesh/scale refinement techniques. The method is successfully applied to elastic materials (Sec. 4) and real burn scar cases (Sec. 5). The last section discusses and summarizes the results of this research.

## 2. BACKGROUND AND MODELING

### 2.1. Ground Truth Estimation Using Mechanics-Based Elasticity Measurements

Elasticity refers to the extent a material changes its length when a force is applied. The *modulus of elasticity*, or Young's modulus, $E$, can be defined as

$$E = \frac{\Delta\sigma}{\Delta\epsilon} \tag{1}$$

where $\Delta\sigma$ is the stress change and $\Delta\epsilon$ is the strain change. The stress, $\sigma$, can be viewed as force per unit area and the strain, $\epsilon$, as changes of lengths per unit length.

To evaluate the performance of the method, we present ground truth elasticity estimation using a conventional approach from mechanics. During the experiments, one end of the object is fixed while variable weights are applied to the other end.

The length of the stretchable part is measured with a micrometer before ($L$) and after the stretching ($L + \Delta L$) to determine change in length ($\Delta L$).

This setup allows for the calculation of stress since dimensions of the material and the weights applied are known. Weight is the force with which gravity "pulls" on an object's mass ($P = mg$, where $P$ is the weight and $g$ is the acceleration of gravity). Strain can be found using Eq. (1)

$$\epsilon = \frac{\sigma}{E} = \frac{P}{AE} \tag{2}$$

or, equivalently, by definition

$$\epsilon = \frac{\Delta L}{L}\,. \tag{3}$$

Hence,

$$\frac{\Delta L}{L} = \frac{P}{AE} \tag{4}$$

and Young's modulus

$$E = \frac{PL}{A(\Delta L)} = \frac{mgL}{A(\Delta L)} \tag{5}$$

where $A$ can be calculated as multiplication of ($a$) width and ($b$) thickness of the material.

However, in the real world complete knowledge of geometry is rare. In computer vision, for example, we can estimate the surface area of the object; however, its thickness might be unknown. In such cases the estimated parameter is not Young's modulus, but rather a number which is the product of Young's modulus and the thickness of the material

$$Eb = \frac{mgL}{a(\Delta L)}\,. \tag{6}$$

Sometimes we want to estimate elasticity of the material embedded into the material with known properties. If the thickness of either material is unknown, we can define a relative elasticity as

$$E_R = \frac{E_2 b_2}{E_1 b_1}\,. \tag{7}$$

Hence, we define properties of the second material in multiples of properties of the first material.

### 2.2. Grid Tracking with Snakes

In computer vision, recognizing objects often depends on identifying particular shapes in an image. Another difficult task is establishing correspondences between the images. The latter facilitates comparisons of similar shapes. Clearly, using an edge detector alone, however good it is, will not separate the object we are looking for from other objects in the image. We need to incorporate more prior knowledge about the grid pattern. For example, in our project we are looking for a burn scar

with the grid stamped on it and trying to follow the deformation of the grid. We know in advance the geometry of the grid, including even the exact number of vertical and horizontal lines. This task can easily be automated. With this much prior knowledge, it is easy to find all of the these lines in the image.

Active contour models, or snakes, allow us to set up such general conditions, and find image structures that satisfy the conditions. A snake is an energy minimizing spline, governed by internal and external forces. It is specified by a set of control points. Each control point has a position, given by $(X, Y)$ coordinates in the image, and a snake is entirely specified by the number and coordinates of its control points. Iterative adjustments to the snakes are made by moving the control points. Williams and Shah[31] provide a fast greedy algorithm for finding the minimum energy contour. They define the total energy of the snake as consisting of the continuity energy, the curvature energy and the image energy

$$E = \int (\alpha(s)E_{\text{cont}}(s) + \beta(s)E_{\text{curv}}(s) + \gamma(s)E_{\text{img}}(s))ds \tag{8}$$

where $s$ denotes the arc-length along the snake. A snake evolves so as to reduce its energy. For more on the general formulation of the energies, see Ref. 13.

The grid used in the experiments consists of a set of intersecting lines. The grid has a lower image intensity than the background which allows to effective evaluate the image energy. Each grid line is tracked by a separate snake. There is a total of seven lines in each of two directions.

A total of six points (selected by the user) are needed to identify the region where initial placement should occur: four corner points and two more points to provide the main direction of stretching. Details are described in Ref. 28. The initialization is necessary for each time frame since the motion is relatively large and it is impossible to know in advance how and where the points move during the stretching.

During the fitting stage, each snake iteratively minimizes its energy to track the exact contour of the corresponding grid line. We move successively from the first snaxel point to the last, shifting each to a new location in its neighborhood where the total energy is a minimum. When the algorithm terminates, the entire set of snakes approximates the shape closely. The last step is computing the intersection points in the images before and after the motion and calculating their 3-D displacements using the corresponding range data. The grid intersection points are computed as the intersection points of the corresponding snakes. These points and their displacements are automatically fed into the FEM model, and provide the foundation for the calculation of motion and deformation parameters.

### 2.3. Nonlinear Finite Element Computation

The elasticity of scarred tissues differs from normal skin. Given the displacements, we attempt to recover strains, forces and relative material properties of tissues within areas of interest.

The basic concept of the finite element method (FEM) is decomposition of a complex object into simpler components called finite elements. The mechanical response of an element is represented in terms of a finite number of degrees of freedom (DOFs). These DOFs are described as the values of the unknown functions at the nodal points. The response of an entire system is then obtained by the discrete model created by assembling the responses of all elements. The advantage of FEM is the possibility of modeling the physics of the material between the nodes. Having a set of material properties for a given object can aid in a precise nonrigid motion tracking of this object.

General *nonlinear* deformation theory defines the displacement field as a combination of rigid-body motions and pure deformations. Rigid-body motions include translations and rotations. Their main property is that the distance between any pair of material points remains unchanged. Any quantity that measures the *change* in length between the neighboring points is a measure of pure deformation. Computationally, incremental approximation (defined in Ref. 9) is used by the ANSYS,[10] program utilized in this research for nonlinear FEM calculation. Increment of the deformation gradient $\Delta G_n$ at the current time step $n$ is defined using the previous time step $n-1$

$$[\Delta G_n] = [G_n][G_{n-1}]^{-1} . \tag{9}$$

### 2.4. Iterative Descent Search

This work utilizes an iterative descent algorithm.[15] *Iterative* means that the algorithm generates series of points, each point being calculated on the basis of points preceding it. *Descent* denotes that as each new point is calculated by the algorithm the corresponding value of some function (evaluated at such point) decreases in value. Any descent algorithm starts at an initial point; determines, according to a fixed rule, a direction of the movement; and then moves in that direction to a minimum of the objective function. Ideally, the sequence of points converges in a finite (or infinite) number of steps to a solution of the original problem. A solution is an extremum (maximum or minimum point). Since we will be estimating an error between the model and the object after the motion, the target of the search is a minimum point.

## 3. METHOD DESCRIPTION

### 3.1. Basic Method

The method (introduced in Refs. 28 and 29) relies on the fact that it is usually harder to pull on a scarred tissue than to pull on normal skin. The nature of skin deformation differs depending on the elasticity of the underlying skin. The basic method consists of three main parts: detection of the grid points with snakes (already described in the previous section), burn scar localization, and an iterative descent search for its material properties (relative to properties of normal skin).

Scar localization is based on the strain analysis of the finite element model of stretching skin. Nonlinear finite element solution is performed in the ANSYS package[10] (version 5.3 on a SUN SPARC 10 with 32 MB of memory) using hyperelastic shell elements with the thickness calculated as a summation of thicknesses of human skin layers (the Epidermis, or outer layer, the Dermis, and the Subcutaneous layer, or lower dermis). If the scar exists in the image, it is found using the level of strain as a criterion. Assuming sufficient stretching to reveal the scar, a sudden change of strain to a minimum reveals the area(s) of the model that correspond to the scar location. This area(s) is the place where we apply an iterative descent search to find its properties relative to properties of normal skin. Absolute properties can be found if the knowledge of precise properties of normal skin for each patient becomes available.

If the material is uniform, both regions stretch the same. Otherwise, the region of greater elasticity contributes much more to the resulting elongation of an entire material. Therefore, if we apply displacements of the boundary points only and vary the value of unknown elasticity, the resulting displacements of the nodes of our FEM model inside the region also change. If we had correct elastic properties for both areas, then the displacements of all of the object's points would have been equal to the motion between two time frames calculated using the available range data. Hence, we can compare new nodal displacements with the base displacements (determined during the detection phase) and estimate the difference that would guide us through the search to the correct value of Young's modulus. The error is computed by comparing true displacements of the nodes (or keypoints) after the motion with a change in positions of nodes predicted by the FEM model incorporating a current hypothesis about Young's modulus of the burn scar. The error is defined per node. Error minimization utilizing the iterative descent method takes place in the neighborhood of the known elasticity. This neighborhood can be defined exactly based on the known properties of the first material and the predicted behavior of the second. The minimum of error function corresponds to the correct elasticity of the second material.

### 3.2. New Method

One of the main contributions of the new method is a possibility to quantify more than two areas in the burn scar region. Since we need to determine differences in these areas as reactions to external forces, the main requirements to apply the method successfully include displacements sufficient to produce such differences. In this case, the strain criterion can pinpoint more than two areas with different elasticities within the grid. The method initially detects two areas — normal and abnormal. If the change of strain is not gradual within either one of these subareas, this indicates a possibility of further subdivision. Very often, in physicians' opinions (see ratings in Sec. 5) the scar consists of multiple low elasticity (or, equivalently, large Young's modulus) areas. The lowest strain can usually indicate the most abnormal area. The next gradation coincides with the somewhat less abnormal area, etc. For example, in our experiments we use nine strain levels. If we define

the lowest strain as strain level one, then level two is present within the abnormal area detected during the previous step.

The iterative descent search method during the current step can proceed using the results of the previous step also in a numerical sense, using the elasticity of the entire abnormal area as a starting point to search for elasticities of subareas. This limits the search space for the new step to achieve the solution faster.

Since some scars do not give in to stretching easily, detection of their shapes might produce various errors. Small propagation of displacements in certain directions can effectively make the outcome unpredictable, reducing or increasing the number of areas composing the burn scar in the model. If the method classifies an additional region as abnormal, the total Young's modulus of the scar decreases since now it represents an average of the real abnormal area and an additional normal area. To prevent such problems, this method proposes the application of different forces in multiple directions. This improvement is especially helpful in better revealing the local geometry of the scar, which can give rise to its better description by scale and mesh refinement of a finite element model.

The term *scale* denotes a level of resolution, or, equivalently, a level of detail. Most objects can be described usefully through a variety of scales. This idea has found use most often as a mechanism to reduce computation: low-cost, low-resolution processing over a coarse grid (applied to the smoothed data) serving to guide high-cost, high-resolution processing over a finer grid. The best result on a coarse scale is the starting point for the next scale. A true scar boundary can lie within one or more model areas, originally classified as completely normal or abnormal. The process proceeds to an accurate solution by splitting up the existing area(s) along the boundary of the scar into multiple areas. This step results in a better description of the boundary and improved classification of model areas.

In order to further minimize the material modeling error we need to specify mesh controls in addition to the above steps. A finer mesh is necessary around the areas of drastic changes in strain. This also usually happens around the boundary between the scar and a normal tissue. *Local mesh refinement*, a common practice described by Burnett,[3] provides additional degrees of freedom in some regions to increase the local accuracy. Based on the automated strategy, the areas with relatively high local error are identified as candidates for remeshing. It is hard to achieve completely automatic meshing based on the given accuracy since the error estimates are difficult and the automatic meshing problem has not been completely solved When the areas are found, their meshing is refined using smaller elements. In general, all domains of the model where the solution tends to be more complicated (e.g. near sharp changes in the shape or concentrated loads) must have meshing of greater density to maintain a given level of accuracy. Of course, mesh refinement changes the number and the assignment of nodes and elements, which requires recalculation of the certain steps of the method, like the node positions from the model based on the range data before and after the motion used to guide the iterative descent search.

Figure 2 shows the steps of the proposed method.

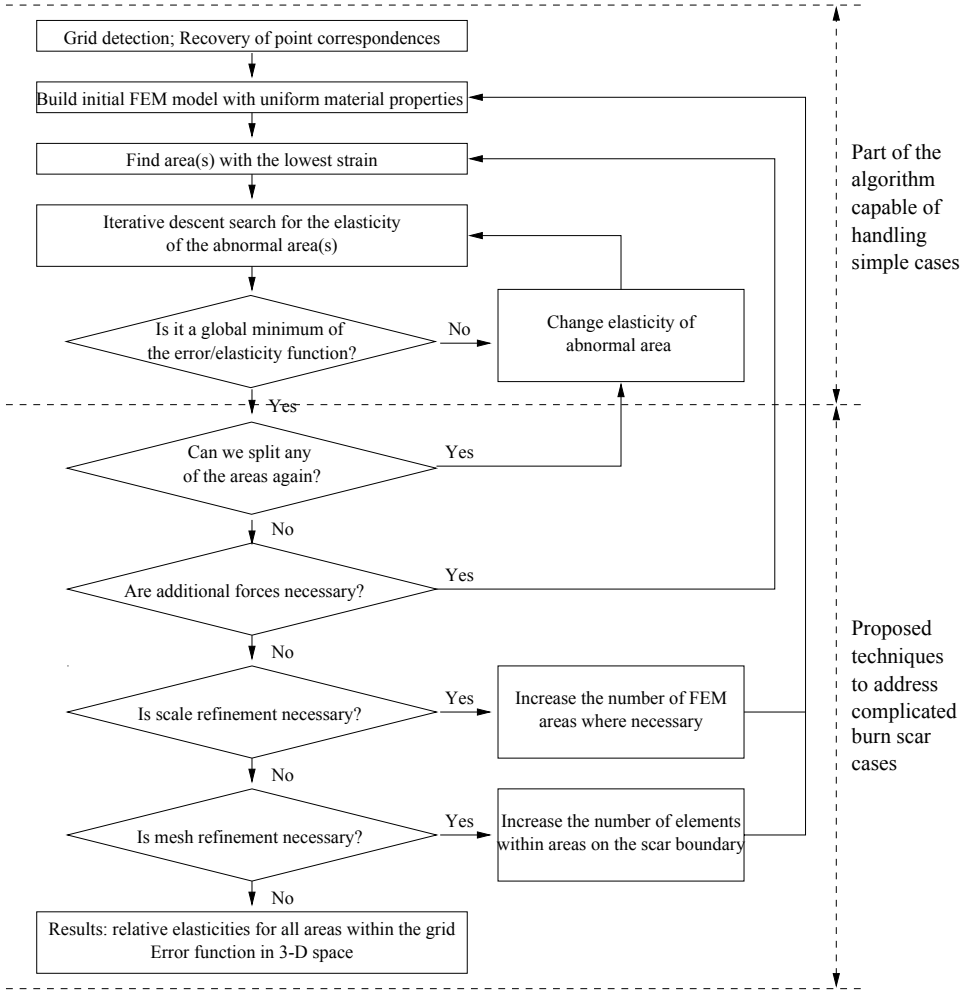


Fig. 2. Algorithm of the new method.

## 4. EXPERIMENTS WITH ELASTIC MATERIALS AND COMPARISON WITH GROUND TRUTH VALUES

Let us analyze the stretching of elastic materials using vision techniques and compare results obtained using a conventional approach from mechanics (Sec. 2.1). We consider experiments with multiple materials of unknown elasticities embedded in a known material. To simulate areas with different properties, rectangular pieces of different materials are attached on top of the initial material. Snakes are used for tracking intersections of the grid stamped on the materials in the images before and after stretching (Figs. 3(a) and 3(b), respectively). The corresponding range image is shown in Fig. 3(c). These intersections function as a set of keypoints for automatic FEM model building. Each grid area is split up into several FEM areas for better precision.

Ground truth values were calculated using Eq. (5). We use elasticities of areas 2 and 3 for validation only. Let us calculate properties of these areas using the proposed method and compare them to the ground truth.

For the initial finite element model, elastic properties are considered to be the same everywhere. The initial model allows us to find displacements of the nodes (base displacements) and the whereabouts of the abnormal areas indicated by the lowest strain levels. Strain, computed as a result of inverse finite element analysis (FEA), is shown in Fig. 3(d). The legend column on the right of the strain distribution shows (top to bottom): maximum displacement, minimum strain (displayed only if it is different from zero) and maximum strain. Nine levels of strain are displayed in the grid area from the lowest (blue) to the highest (red). The next step is to search for values of unknown properties using an iterative descent algorithm based on the difference between resulting nodal displacements and base (real) displacements.

Results of the basic method are shown in Table 1. An iterative search error is down from $1763.18(10^{-6})$ m to $677.16(10^{-6})$ m, however, the difference with ground truth is 262% for area 2 and 27% for area 3. The reason for this is the inability of the old method to handle multiple unknown areas.

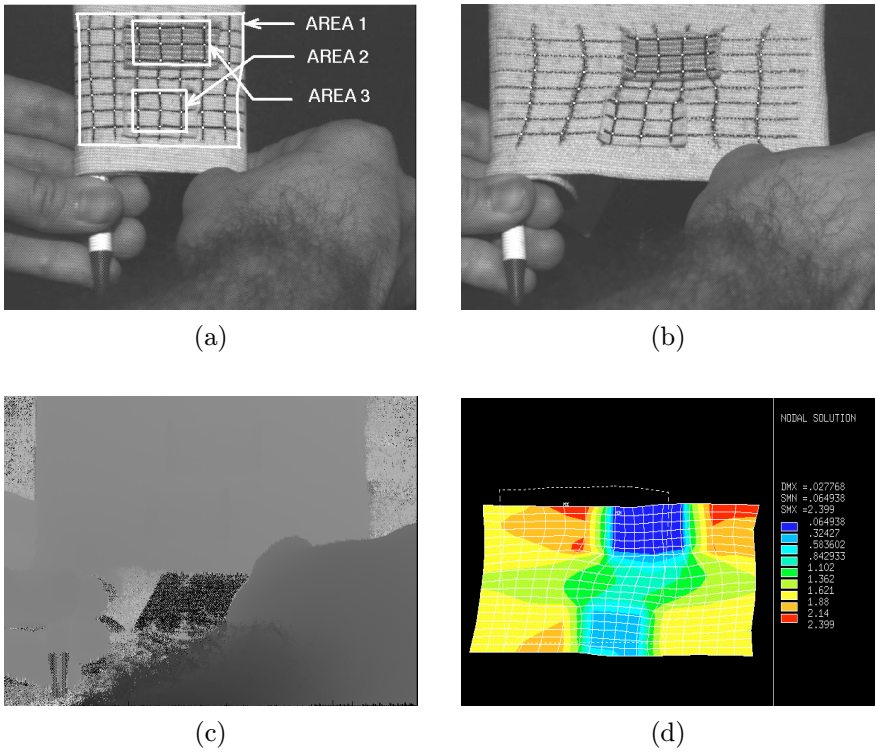


Fig. 3. Experiments with elastic materials. (a–b) Snake detection of the grid before and after stretching. (c) The range image of the skin after stretching. (d) Resulting strain distribution. Nine levels of strain are displayed in the grid area from the lowest (blue) to the highest (red).

Table 1. Comparison of resulting properties of abnormal areas recovered by old and new methods.

| Area number | Ground truth, kPa | Results of the old method, kPa | Difference, % | Search error/node, $10^{-6}$ m | Results of the new method, kPa | Difference, % | Search error/node, $10^{-6}$ m |
|---|---|---|---|---|---|---|---|
| 2 | 335.04 | 1214.52 | 262.5 | 677.16 | 343.42 | 2.5 | 577.64 |
| 3 | 1675.20 | 1214.52 | 27.5 | 677.16 | 1725.46 | 3.0 | 577.64 |

The new method considers three separate areas, and iterates until a minimum in this 3-D space is found ($577.64(10^{-6})$ m). The difference with ground truth now does not exceed 3%. Table 1 proves that the results of the new method are, indeed, very precise.

If we assume that elasticity of area 1 is unknown, we can estimate relative properties of areas 2 and 3 in multiples of properties of area 1 (as defined in Eq. (7): 4.1 for area 2 and 20.6 for area 3). This is what we recover in burn scar assessment procedure. In our experiments precise skin and burn scar thickness and precise elasticity of normal skin are not practical to estimate for each patient because of *in-vivo* nature of the experimental setup. Using relative elasticity (7) is sufficient to determine the success of treatment (increase in elasticity of burn scar relative to the surrounding areas).

The next section will illustrate the application of the proposed method to complicated burn scar cases and show other advantages of the method, including utilization of multiple forces and scale/mesh refinement techniques.

## 5. EXPERIMENTAL RESULTS OF BURN SCAR ASSESSMENT

### 5.1. Multiple Abnormal Areas

Let us look at a very interesting series of experiments demonstrating the superiority of the method when given sufficient data to apply all of the steps. This case introduces a large scar on the arm that allows for a significant stretching sufficient to reveal skin properties. Figures 1(a) and 4(a) show the gray-level intensity images of this patient's skin on the arm before and after stretching, respectively. The range image corresponding to Fig. 1(a) is shown in Fig. 1(b). The grid detection part is displayed in Fig. 4(b).

The change in length in this case (detected in the direction of stretching) comprises about 17% of the original length. Unfortunately, some cases are limiting change in length to 7% at the most. This means that stretching is the predominant motion of skin which is crucial for the method since our model simulates only stretching behavior of skin (as opposed to bending, compressing, or pushing perpendicularly to the surface of the arm).

The basic method reveals abnormalities in the grid area. However, this time all of the strains produced are caused solely by the effect of stretching on the skin with different elastic properties. Therefore, strain gradation is sufficient to reveal gradations within the abnormal area. For instance, in Fig. 5(a) two definite areas are found within the abnormal area (the entire right part of the model) — one in

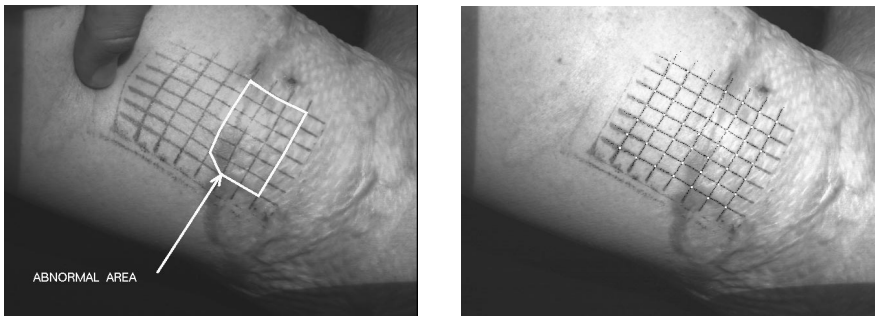


(a) (b)

Fig. 4. (a) The intensity image of the skin with the grid. The abnormal area is outlined by the physician. (b) Detecting the grid using snakes.

the lower part (more abnormal as described by the strain legend on the right) and the other in the upper part (less abnormal).

However, for now we treat both detected abnormal areas as one. Initially the method proceeds like before by iterating until the minimum error is found [Fig. 5(b)]. The resulting elasticity for the abnormal area is 2.5 [Fig. 6(a)]. 2.5 is the ratio of elasticities of abnormal and normal areas. The subdivision within the abnormal area is still clear from this result.

The new method continues by searching for a possible split within normal or abnormal areas separately. We already discovered that the area, indicated initially [Fig. 5(a)] by the lowest strain, is less elastic (the top box in the legend) and that the rest of the abnormal area (the second box from the top) is slightly more elastic (but still less, compared to the normal skin for this patient). Therefore, we have three areas to analyze — one normal and two abnormal. Would introducing the third area really improve the result? To demonstrate it, we can investigate the set of functions [Fig. 6(b)].

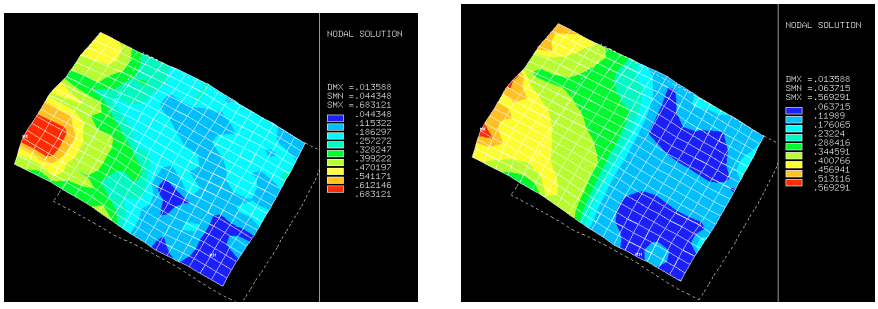


(a) (b)

Fig. 5. Results (strain distributions) using old method. (a) Initial detection of abnormal area when its properties are unknown. (b) Result of iterative descent assuming two areas within the grid.

Each of these functions represents error function between the model and range image data when we vary the elasticity of the more abnormal area while the elasticity of the less abnormal area is fixed (a different number for each function). The difference between these functions is obvious. Although some of them exhibit higher errors at the points limiting boundary intervals [up to $550(10^{-6})$ m verses about $370(10^{-6})$ m in Fig. 6(a)], the minimum has smaller value than the best previous iteration [lower than $250(10^{-6})$ m as opposed to higher than $260(10^{-6})$ m before].

Hence, the process is extended so that we continue by splitting the abnormal area into two, and continuing the iterations until the minimum error is located in this 3-D search space. This step is directly based on the results of the previous step because bounding intervals for both unknown elasticities are located in the neighborhood of 2.5. This fact limits the search space and time. The results are 3 and 2.4 (again, one is considered a normalized modulus elasticity for normal skin). The strain map corresponding to the final result is shown in Fig. 6(c). This is remarkably similar to the rating by a physician [Fig. 6(d)] if we consider a scaling factor determined

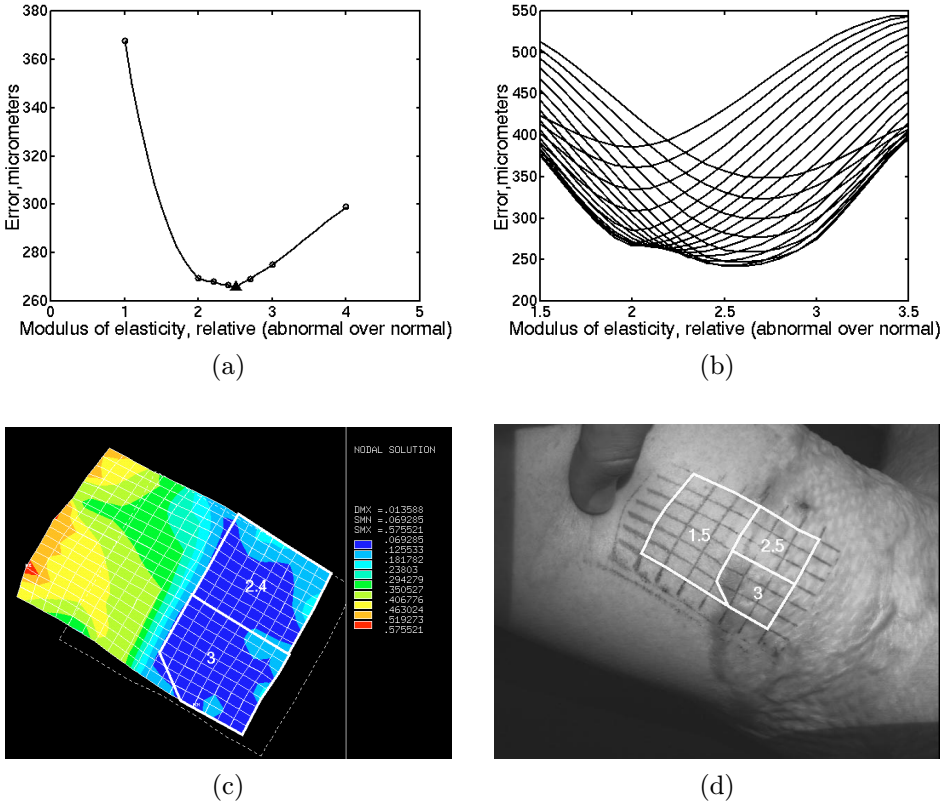


Fig. 6. Elasticity functions and results using updated method. (a) Elasticity function. (b) Multiple functions error versus elasticity of more abnormal area when elasticity of less abnormal area is fixed. (c) Result of iterative descent after the subdivision of abnormal area. (d) Rating by a physician. Physicians rate elasticity of burn scars on a scale from 1 (normal) to 5 (extreme decrease in elasticity).

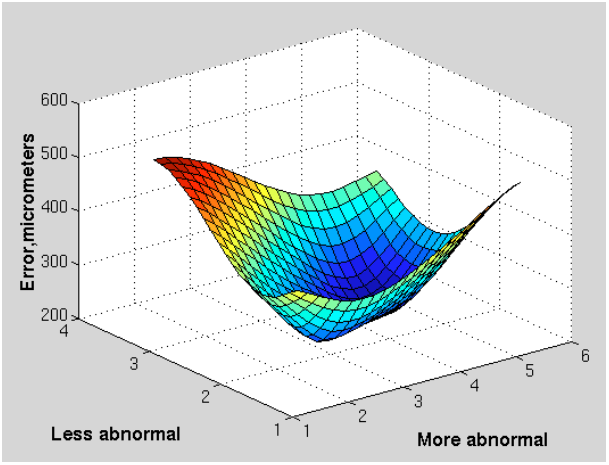


Fig. 7. Three-dimensional error function. The error depends on the variation of both unknown elasticities (indicated as less abnormal and more abnormal).

empirically. Physicians rate elasticity of burn scars on a scale from 1 (normal) to 5 (extreme decrease in elasticity). Our method also found two abnormal areas and correctly rated them according to their properties. To verify numerical results, we have to divide our results by the scaling factor of 1.5 (demonstrated for 15 burn scar sequences in Refs. 28 and 29): $3/1.5 = 2$ and $2.4/1.5 = 1.6$. Physicians' rating is also relative (abnormal over normal), hence the relative elasticity of more abnormal area is $3/1.5 = 2$, and the relative elasticity of less abnormal area is $2.5/1.5 = 1.67$. This demonstrates a direct correlation between two sets of ratings.

The final 3-D elasticity function, in which an additional dimension represents a new (less elastic) area found within the scar, is represented in Fig. 7. The error depends on the variation of both unknown elasticities (indicated as less abnormal and more abnormal). The function has only one minimum, similarly to investigated 2-D error functions.

### 5.2. Multiple Forces in Different Directions and Scale/Mesh Refinement

If we look more carefully at the results of the previous experiment, we will notice that a very small local variation in the shape of the scar was not properly captured by the model. The basic method was rather oriented at the recovery of the general location and elastic modulus of the scar. Additional techniques are introduced to estimate complex shapes better. The following experiments attempt to address this extension.

Now let us illustrate what happens when multiple stretching forces are applied in different directions [Fig. 8(a)]. The shape of the abnormal area detected during the first step of the method is slightly different [Fig. 8(b)] because the force at the bottom of the grid affects this part much more than stretching in the previous setup. The search for elasticity of abnormal areas proceeds similarly by finding one combined number and then continuing for separate abnormal areas within the scar

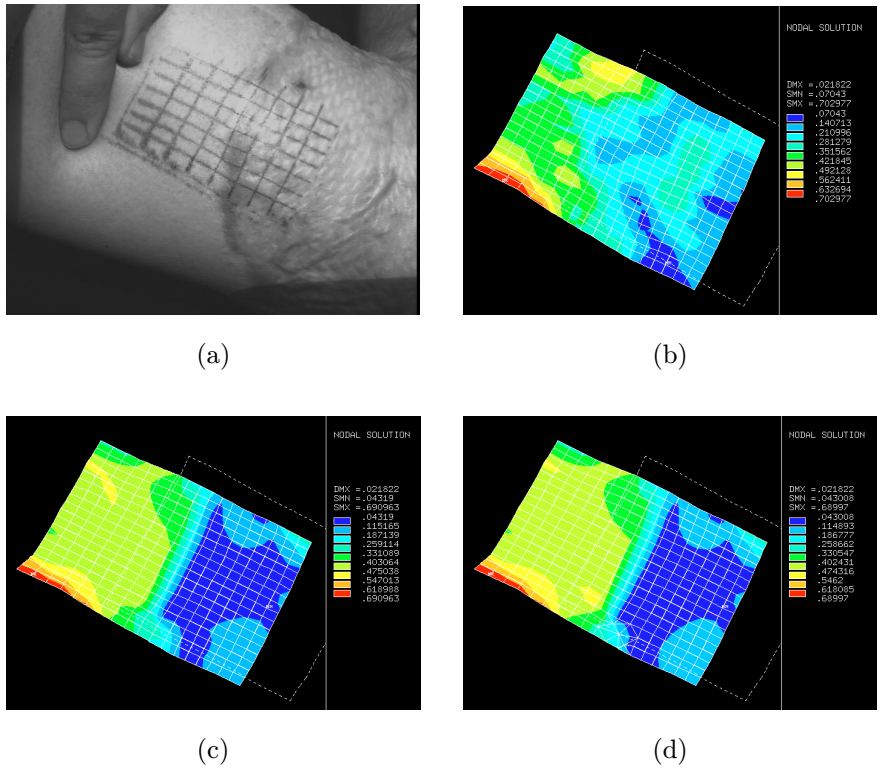


Fig. 8. (a) Multiforce stretching. (b) Result of the first step (initial detection). (c) Final result (relative elasticity recovered and area localized). (d) Local refinement integrated into the method.

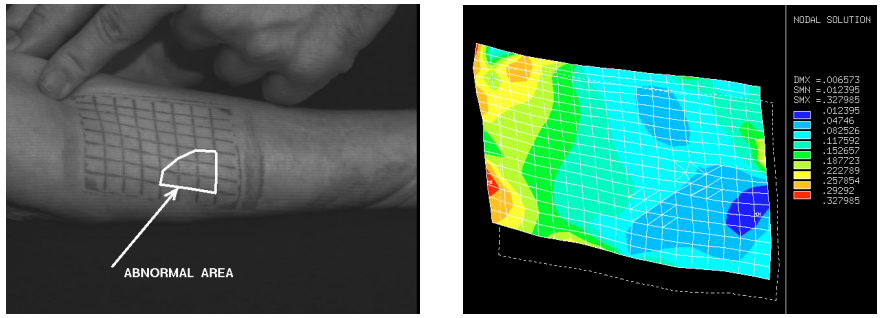


Fig. 9. (a) The intensity image of the burn scar (another patient). (b) Result with local scale and mesh refinement based on a given scar boundary.

[Fig. 8(c)]. Although the shape of the more abnormal area is captured much better now, it is still a bit far from a more precise description as suggested by the strain map [Fig. 8(b)]. The final touch is done by a local scale and mesh refinement in the area where we want to increase the precision of scar shape interpretation [Fig. 8(d)].

This step improves precision of the detection as well as of the elasticity search.

Scale and mesh refinement can be done even in more complicated cases. For instance, if the strain cannot reveal the need for a local refinement, but the burn scar boundary is given, then the improvement is still clear. Figure 9 shows the results for another patient when the refinement was applied based on the boundary indicated on the intensity image by a physician. The resulting elasticity is 3.1 which again correlates to a judgment by a physician (when difference in scales is considered).

### 5.3. Reasons for Having Deviations — Anisotropism and Variable Thickness

Multiple rankings of the same patient by the same or different physicians have shown that human assessment of burn scar elasticity is in fact extremely subjective (up to 50% difference in elasticity estimation). Why do the results of our method differ slightly from execution to execution? We need to mention that an iterative search procedure is very robust. However, detection of location and shape of the burn scar can be affected by various factors. First, it can be influenced by the noise that has been analyzed with thresholds and already explained in detail in Ref. 29. Second, a relatively small elongation may produce insufficient input from stretching in the resulting strain map. The strain map influences the selection of an abnormal area. If a selected area is smaller than the real area, then the result is different from a true Young's modulus of this area since it attempts to compensate for observed stretching. Most importantly, what can cause the small result deviation for such reliable data as in the cases described in Secs. 5.1 and 5.2?

The answer lies in the nature of burn scars themselves, specifically in anisotropicity of elastic properties and in variations of scar thickness. The imaginary line which defines the direction of external force intersects parts of the scar with different thicknesses. If the thickness is unknown, then the result of our method is a product of the elasticity of abnormal area and the ratio of its thickness and the thickness of normal area (as defined in Eq. (7)). Therefore this result can differ for different force directions since the scar thickness is not constant. Pulling along the thicker part of the scar produces a greater result.

Experiments also show that soft tissues are anisotropic, especially burn scar regions. That is why variation of directional components of Young's modulus influenced the error. For example, more abnormal part of the scar in Fig. 4 resulted in our rating of 3 ($E = 3$). However, when we extended the search to find directional components of Young's modulus, results were: $E_y = 3$ and $E_x = 3.9$. Reduction in the total error was not very significant, which can be explained by the nature of our experimental setup based on the unidirectional stretching. How much anisotropicity and thickness influence the result with respect to each other has yet to be determined.

## 6. DISCUSSION AND CONCLUSIONS

In this paper we proposed a method for increasing precision and reliability of elasticity analysis in complicated burn scar cases. The new method can split the region

into more than two localities with different material properties, select and quantify abnormal areas, and apply different forces if it is necessary for a better shape description of the scar. The method also demonstrates the application of scale and mesh refinement techniques in this important domain. It is accomplished by increasing the number of FEM areas as well as the number of elements within the area.

The method was successfully applied to elastic materials and real burn scar cases. We demonstrated all of the proposed techniques and investigated the behavior of elasticity function in a 3-D space. Recovered properties of elastic materials were compared with those obtained by a conventional mechanics-based approach. Scar ratings achieved with the method were correlated against the judgments of specialists.

We have applied the proposed method to our database consisting of 72 image sequences, including image sequences of elastic materials (from one to three different elasticities), image sequences of normal skin, burn scars and simulated skin abnormalities. Table 2 demonstrates the success of different parts of the method. The split into normal and abnormal areas requires sufficient differences in displacements in these areas. To detect additional abnormal (or normal) areas, these displacements must produce an evidence that a new candidate area contrasts from already classified areas. Therefore as more data is being acquired, we are including this important condition as necessary for the experimental setup.

Table 2. Summary of results.

| Experiment type | More than one abnormal area detected and quantified | Additional forces applied | Refinement applied |
|---|---|---|---|
| Elastic materials | 7 | 7 | 0 |
| Burn scars | 5 | 8 | 7 |
| Total | 12 | 15 | 7 |

Would the modeling error function in 3-D space always have one minimum? The experiments show that if additional minimums are introduced, they can be eliminated by using additional local error estimates within each detected area.

This method will be utilized for the quantitative assessment and comparison of burn scar treatment results. The method will allow us to estimate the progress in scar healing as a function of the difference in its elastic properties as they approach elastic properties of the normal skin.

## REFERENCES

1. A. A. Amini, Y. Chen, R. W. Curwen, V. Mani and J. Sun, "Coupled b-snake grids and constrained thin-plate splines for analysis of 2d tissue deformations from tagged MRI," *IEEE Trans. Med. Imag.* **17**, 3 (1998) 344–356.

2. S. Basu and A. Pentland, "A three-dimensional model of human lip motions trained from video," *IEEE Nonrigid and Articulated Motion Workshop*, San Juan, Puerto Rico, June 1997, pp. 46–53.
3. D. S. Burnett, *Finite Element Analysis*, Addison-Wesley Publishing Company, 1988.
4. S. Chandran and A. K. Potty, "Energy minimization of contours using boundary conditions," *IEEE Trans.* **PAMI-20**, 5 (1998) 546–549.
5. M. H. Davis, A. Khotanzad, D. P. Flamig and S. E. Harms, "A physics-based coordinate transformation for 3-d image matching," *IEEE Trans. Med. Imag.* **16**, 3 (1997) 317–328.
6. D. DeCarlo and D. Metaxas, "Adaptive shape evolution using blending," *Proc. 5th Int. Conf. Computer Vision*, Boston, MA, June 1995, pp. 834–839.
7. Y. C. Fung, *Biomechanics: Mechanical Properties of Living Tissues*, 2nd edition, Springer-Verlag, NY, 1993.
8. S. R. Gunn and M. S. Nixon, "A robust snake implementation; a dual active contour," *IEEE Trans. Patt. Anal. Mach. Intell.* **19**, 1 (1997) 63–68.
9. T. J. R. Hughes, "Numerical implementation of constitutive models," *Theoretical Foundation for Large-Scale Computations for Nonlinear Material Behavior*, Dordrecht, The Netherlands, 1984, Martinus Nijhoff Publishers.
10. Inc. Swanson Analysis System. *ANSYS User's Manual for Revision 5.3*, Swanson Analysis System, Inc., Houston, PA, 1996.
11. M. Kass, A. Witkin, and D. Terzopoulos, "Snakes: active contour models," *Int. J. Comput. Vis.* **1**, 4 (1998) 321–331.
12. F. Kallel and M. Bertrand, "Tissue elasticity reconstruction using linear perturbation method," *IEEE Trans. Med. Imag.* **15**, 3 (1996) 299–313.
13. S. Kumar and D. B. Goldgof, "Automatic tracking of SPAMM grid and the estimation parameters from Cardiac MR images," *IEEE Trans. Med. Imag.* **13**, 1 (1994) 122–132.
14. W. F. Larrabee and J. A. Galt, "A finite element model of skin deformation. III. The finite element model," *Laryngoscope* **96** (1986) 413–419.
15. D. Luenberger, *Linear and Nonlinear Programming*, Addison-Wesley, Reading, MA, 1984.
16. J. Martin, A. Pentland, S. Sclaroff and R. Kikinis, "Characterization of neuropathological shape deformations," *IEEE Trans.* **PAMI-20**, 2 (1998) 97–112.
17. J. C. McEachen, II and J. S. Duncan, "Shape-based tracking of left ventricular wall motion," *IEEE Trans. Med. Imag.* **16**, 3 (1997) 270–283.
18. A. A. McHugh, B. J. Fowlkes, E. I. Maevsky, D. J. Smith Jr., J. L. Rodriguez and W. L. Garner, "Biomechanical alterations in normal skin and hypertrophic scar after thermal injury," *J. Burn Care and Rehabilitation* **18** (1997) 104–108.
19. D. Metaxas and E. Koh, "Efficient shape representation uisng deformable models with locally adaptive finite elements," *SPIE Vol. 2031, Geometric Methods in Computer Vision II*, San Diego, CA, July 1993, pp. 160–171.
20. D. Metaxas and D. Terzopoulos, "Constrained deformable superquadrics and nonrigid motion tracking," *Proc. IEEE Conf. Computer Vision and Pattern Recognition*, Hawaii, 1991, pp. 337–343.
21. P. S. Powers, S. Sarkar, D. B. Goldgof, C. W. Cruse and L. V. Tsap, "Scar assessment: current problems and future solutions," *J. Burn Care and Rehabilitation* **20**, 1 (1999) 54–60.
22. S. Sclaroff and A. P. Pentland, "Physically-based combinations of views: representing rigid and nonrigid motion," *Proc. 1994 IEEE Workshop on Motion of Non-Rigid and Articulated Objects*, Austin, TX, November 11–12, 1994, IEEE Press, pp. 158–164.
23. A. Singh, D. B. Goldgof and D. Terzopoulos (eds.), *Deformable Models in Medical Image Analysis*, IEEE Computer Society Press, Los Alamitos, CA, 1998.

24. T. Sullivan J. Smith, J. Kermode, E. McIver and D. J. Courtemanche, "Rating the burn scar," *J. Burn Care and Rehabilitation* **11** (1990) 256–260.
25. H. D. Tagare, "Deformable 2-d template matching using orthogonal curves," *IEEE Trans. Med. Imag.* **16**, 1 (1997) 108–117.
26. D. Terzopoulos and K. Waters, "Analysis and synthesis of facial images using physical and anatomical models," *IEEE Trans. Patt. Anal. Mach. Intell.* **14**, 6 (1993) 569–579.
27. L. V. Tsap, D. B. Goldgof, S. Sarkar and W.-C. Huang, "Efficient nonlinear FEM modeling of nonrigid objects via optimization of mesh models," *Special Issue of Comput. Vis. Imag. Understanding on CAD-Based Computer Vision* **69**, 3 (1998) 330–350.
28. L. V. Tsap, D. B. Goldgof, S. Sarkar and P. Powers, "Experimental results of a vision-based burn scar assessment technique," *Proc. IEEE Workshop on Biomedical Image Analysis (WBIA'98)*, Santa Barbara, CA, June 1998, pp. 193–201.
29. L. V. Tsap, D. B. Goldgof, S. Sarkar and P. Powers, "A vision-based technique for objective assessment of burn scars," *IEEE Trans. Med. Imag.* **17**, 4 (1998) 620–633.
30. J. A. Weiss, J. A. Painter and E. P. France, "Finite element mesh generation of the knee and its soft tissues from CT data," *Proc. 2nd World Congress of Biomechanics*, Amsterdam, The Netherlands, July 1995, p. 149.
31. D. J. Williams and M. Shah, "A fast algorithm for active contours and curvature estimation," *CVGIP: Imag. Understanding* **55**, 1 (1992) 14–26.
32. A. Yezzi, Jr., S. Kichenassamy, A. Kumar, P. Olver and A. Tannenbaum, "A geometric snake model for segmentation of medical imagery," *IEEE Trans. Med. Imag.* **16**, 2 (1997) 199–209.
33. A. Young and L. Axel, "Non-rigid wall motion using MR tagging," *Proc. Computer Vision and Pattern Recognition*, Champaign, IL, June 1992, pp. 399–404.

**Leonid V. Tsap** received the B.S. degree in computer science from the Kiev Civil Engineering Institute, Ukraine, in 1991, and the M.S. and Ph.D. degrees in computer science from the University of South Florida, Tampa, in 1995 and 1999, respectively. He also held full-time professional positions ranging from computer programmer to senior analyst, and taught a number of classes at USF. He is a three-time winner of the annual University of South Florida USPS Scholarship Award, and a recipient of the Provost's commendation for outstanding teaching by a graduate student. He is currently with the Center for Applied Scientific Computing at the Lawrence Livermore National Laboratory.

Leonid V. Tsap is a member of the IEEE Computer Society and ACM. His current research interests include gesture tracking and recognition, modeling of biological materials and man-made nonrigid objects, image analysis/computer vision, image synthesis and visualization, elasticity analysis, model parameter optimization and biomechanics. His recent research projects and conference presentations as shockwave movies can be found at http://marathon.csee.usf.edu/~tsap.

**Dmitry B. Goldgof** received the M.S. and Ph.D. degrees in electrical engineering from the Rensselaer Polytechnic Institute in 1985 and the University of Illinois, Urbana-Champaign, in 1989, respectively. He is currently an Associate Professor in the Department of Computer Science and Engineering at the University of South Florida.

Professor Goldgof's research interests include motion analysis of rigid and nonrigid objects, computer vision, image processing and its biomedical applications, and pattern recognition. Dr. Goldgof has published over 35 journal and 80 conference publications, 8 book chapters and one book. He is currently a member of the Editorial Board of the *Pattern Recognition* and *North American Editor for Image and Vision Computing Journal.* Dr. Goldgof recently completed his term as an Associate Editor for IEEE Transactions on Image Processing. Dr. Goldgof has served as a General Chair for IEEE Conference on Computer Vision and Pattern Recognition (CVPR'98) and as an Area Chair for CVPR'99.

Dr. Goldgof is a senior member of IEEE, member of the IEEE Computer Society, IEEE Engineering in Medicine and Biology Society, SPIE — The International Society for Optical Engineering, Pattern Recognition Society, and the Honor Societies of Phi Kappa Phi and Tau Beta Pi. More information can be obtained from his home page: http://marathon.csee.usf.edu/goldgof/

**Sudeep Sarkar** received the B.Tech degree in electrical engineering from the Indian Institute of Technology, Kanpur, in 1988 where he was judged the best graduating electrical engineer. He received the M.S. and Ph.D. degrees in electrical engineering, on a University Presidential Fellowship, from the Ohio State University, Columbus, in 1990 and 1993, respectively. Since 1993, he has been with the Computer Science and Engineering Department at the University of South Florida, Tampa, where he is currently an Associate Professor. He is the recipient of the National Science Foundation CAREER award in 1994, the USF Teaching Incentive Program Award for undergraduate teaching excellence in 1997 and the Outstanding Undergraduate Teaching Award in 1998. He is the co-author of the book *Computing Perceptual Organization in Computer Vision*, published by World Scientific. He is also the guest co-editor of the *Computer Vision and Image Understanding* (*CVIU*) *Journal*, Special Issue on Perceptual Organization in Computer Vision, Oct 1999. He is presently serving on the editorial boards for the *IEEE Transactions on Pattern Analysis and Machine Intelligence*, *Journal of Pattern Recognition*, and *Pattern Analysis and Applications Journal*.

His research interests include perceptual organization in single images and multiple image sequences, probabilistic reasoning, Bayesian Networks, low-level image segmentation, color-texture analysis of burn scars, non-rigid modeling of impact of burn scars, and performance evaluation of vision systems.

His recent research projects are listed at http://marathon.csee.usf.edu/sarkar/sarkar.html

**Pauline Powers**, Professor of Psychiatry, College of Medicine, University of South Florida, is responsible for the coordination of the department's clinical, research and training programs in Psychosomatic Medicine. As part of these responsibilities, she directs and oversees its specialized programs in anorexia nervosa and other eating disorders and is Psychiatric Consultant to the Tampa General Hospital Burn Program. Dr. Powers received her M.D. degree from the University of Iowa in 1971 and completed her residency in Psychiatry at the University of California at Davis in 1975. She is certified by the American Board of Psychiatry and Neurology. She has been a member of the faculty at U.S.F. since 1975.

*Photograph of Pauline Powers is unavailable.*